JCS–Japan

EXPRESS LETTER

Study on properties of $BaZr_{0.7}Ce_{0.2}Y_{0.1}O_{3-\delta}$ ceramics prepared by high-pressure sintering

Jiazhuo PENG[1], Heping LI[1,†] and Sen LIN[1]

[1] Key Laboratory of High-temperature and High-pressure Study of the Earth's Interior, Institute of Geochemistry, Chinese Academy of Sciences, 99 West Lincheng Road, Guiyang 550081, P. R. China

High-pressure sintering method was used to prepare the proton conductor based on $BaZr_{0.7}Ce_{0.2}Y_{0.1}O_{3-\delta}$ for the first time, and a comparative research of traditional pressureless sintering and high-pressure sintering methods was carried out. High-pressure sintering accelerated the sintering densification and greatly lowered the sintering temperature, resulting in high performance $BaZr_{0.7}Ce_{0.2}Y_{0.1}O_{3-\delta}$ product which was expected to be used as solid electrolyte to fabricate a sensor for measuring hydrogen in high-pressure hydrothermal systems.

In recent years, high temperature proton conductors (HTPC) have been intensively studied because of their actual and potential application in many fields (e.g. hydrogen sensors, fuel cells and electrochemical reactors).[1] Among all the HTPC, $BaCeO_3$-based proton conductors show the highest proton conductivity;[2] unfortunately, they are not chemically stable in CO_2 and H_2O containing atmospheres.[3,4] In contrast, $BaZrO_3$-based proton conductors show better chemical stability;[5] however, they exhibit poor sinterability and lower protonic conductivity.[6,7] Accordingly, an eclectic method has been proposed for obtaining solid solution containing both $BaCeO_3$ and $BaZrO_3$ to couple high conductivity and good stability.[8]–[10]

The most essential issue that needed to be urgently solved for in-situ monitoring of hydrogen in high-pressure hydrothermal systems (HPHS) is to seek a suitable electrolyte material which has high proton conductivity and is extremely resistant to severe mechanical, thermal, and chemical conditions. The emergence of $BaCeO_3$–$BaZrO_3$ solid solution materials provide a new thought to handle the tough issue.[11] Nevertheless, it should be pointed out that the preparation of $BaCeO_3$–$BaZrO_3$ solid solution by traditional methods requires exceedingly high sintering temperatures (>1600°C) and long dwell times (>10 h); these may lead to barium evaporation and proton conductivity decrease.[8,12] Besides that, the chemical and physical conditions of high-pressure hydrothermal fluids are so extreme that proton conductors prepared by traditional methods cannot already satisfy the strict requirements for use in this environment.

Therefore, it is essential to develop new methods to obtain high performance proton conductors that can be used in high-pressure hydrothermal fluids. In the present work, we present a new method to prepare high performance $BaZr_{0.7}Ce_{0.2}Y_{0.1}O_{3-\delta}$ (BZCY) ceramics. The comparison and analysis between the new and traditional methods are carried out.

$BaCO_3$ (99.95%), ZrO_2 (99.95%), CeO_2 (99.95%) and Y_2O_3 (99.99%) were used for the synthesis of $BaZr_{0.7}Ce_{0.2}Y_{0.1}O_{3-\delta}$ powders by high temperature solid state reaction at 1350°C for 12 h. The synthesized powders were pressed into pellets (8 mm in diameter and 6 mm in thickness) at 250 MPa and then sintered by traditional pressureless sintering at 1650°C for 20 h and high-pressure sintering at 1200°C/1 GPa for 1 h, respectively. The high-pressure sintering was performed on a DS 6 × 1400 t cubic press, and the sample assembly was presented in **Fig. 1**. The densities of sintered pellets were determined by a water immersion (Archimedes) method, which showed the BZCY prepared by pressureless sintering was only about 89% of the theoretical density, whereas that high-pressure sintered BZCY had a high density, ~96%.

The sintered ceramics were ground into circular truncated cone by universal cylindrical grinder and then mounted on an autoclave plug containing conical-hole for HPHS test. A quarter of cavities in the autoclave was covered by deionized water, and HPHS formed after heating. Temperature and pressure inside autoclave were monitored by K-type thermocouple and digital pressure sensor, and the values were transmitted to the computer and recorded. The phase compositions and microstructures of the sintered BZCY samples before and after HPHS test were examined using X-ray diffraction (XRD, Empyrean,

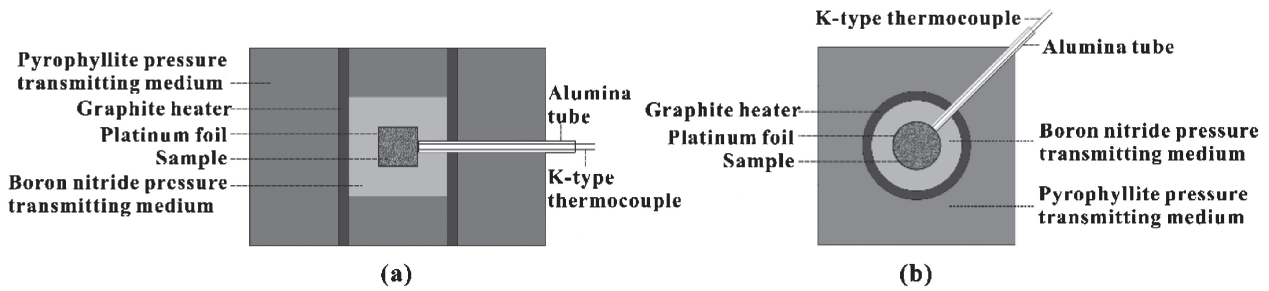† Corresponding author: H. Li; E-mail: liheping@vip.gyig.ac.cn

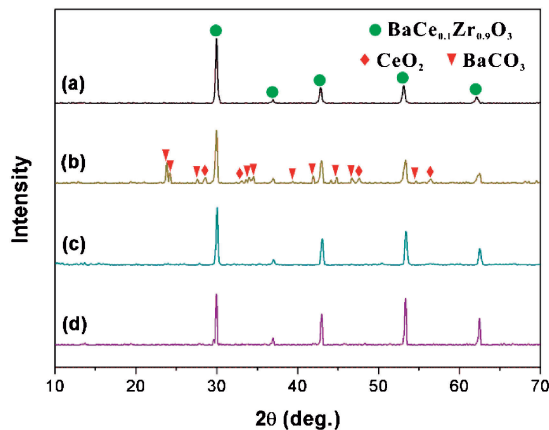Fig. 1. Sectional view (a) and vertical view (b) of the sample assembly.

Fig. 2. XRD patterns of pressureless sintered BZCY pellets before (a) and after (b) HPHS test, and high-pressure sintered BZCY pellets before (c) and after (d) HPHS test.

Holland) and scanning electron microscope (SEM, JSM-7800F, Japan), respectively.

XRD patterns of BZCY samples sintered at 1650°C for 20 h and 1200°C/1 GPa for 1 h are presented in **Figs. 2**(a) and 2(c), all these diffraction peaks could be indexed to the standard powder diffraction file of $BaCe_{0.1}Zr_{0.9}O_3$ (JCPDS No. 70-3668), indicating that pure phase BZCY samples with good crystallinity were successfully prepared by both pressureless and high-pressure sintering methods. Figures 2(b) and 2(d) show the XRD patterns of the pressureless and high-pressure sintered BZCY samples after 24 h testing in HPHS at 400°C/28 MPa, the XRD patterns of the high-pressure sintered BZCY samples were almost the same before and after HPHS test, demonstrating that the BZCY samples obtained by high-pressure sintering exhibit excellent chemical stability. However, the characteristic peaks of $BaCO_3$ and CeO_2 besides BZCY were observed in the patterns of pressureless sintered BZCY samples after HPHS test, showing that some chemical reactions occurred in the BZCY samples during HPHS test.

Figures 3(a) and 3(b) show the SEM images of the pressureless sintered BZCY samples before and after HPHS test, there were a few large pores in the samples, and the average grain size was about 0.5 µm. Furthermore, the grains of the samples after HPHS test were in various shapes such as fibrous, columnar or flaky, and the distribution of grain size was inhomogeneous. The SEM pictures of high-pressure sintered BZCY samples before and after HPHS test are presented in Figs. 3(c) and 3(d), the high-pressure sintered BZCY samples were fully dense with an average grain size about 10 µm, and exhibited less porosity and bigger grains compared to pressureless sintered BZCY samples. There was hardly any difference in the microstructures of high-pressure sintered BZCY samples before and after HPHS test, except the crystalline grains of the samples ware clearer after HPHS test, which might be due to the corrosion of grain boundaries by high-pressure hydrothermal fluids. The results of micromorphology observation were consistent with those of XRD analysis that better chemical and thermal stability for high-pressure sintered BZCY samples compared to pressureless sintered BZCY samples.

The schematic diagram of the experimental setup for HPHS test is shown in **Fig. 4**(a), the sintered BZCY samples were processed into circular truncated cone and assembled into a water-filled autoclave as sealing materials. Heating the autoclave creates a rising pressure as long as the BZCY sample can withstand the impact of high-pressure hydrothermal fluid; otherwise the pressure will not rise. Figures 4(c) and 4(d) show the pressure-time curves of the autoclave when pressureless and high-pressure sintered BZCY samples were used as sealing materials, combining with the temperature-time curve of Fig. 4(b), the sealing performance of the sintered BZCY samples can be tested. When high-pressure sintered BZCY sample was used as sealing material, the change trend of pressure-time curve was consistent with that of temperature-time curve, and the pressure in the autoclave was about 28 MPa at the highest temperature (400°C). Sample was taken out after HPHS test, and it was found that the sample was intact and not damaged. The pressure resistance of high-pressure sintered BZCY was tested by an universal testing machine, and the result showed that its compressive strength was about 279 MPa. However, when pressureless sintered BZCY sample was used as sealing material, the change trend of pressure-time curve was quite different from the temperature-time curve, and the pressure in the autoclave rose at first as the temperature increased and then fell to normal pressure after the pressure reached 1.5 MPa. After the HPHS test, it was found that the sample had broken into small fragments. The process of material failure was caused by stress corrosion. There are a lot of pores in the BCZY sample prepared by pressureless sintering. Affected by stress together with corrosion medium, cracks first appear on the surface of
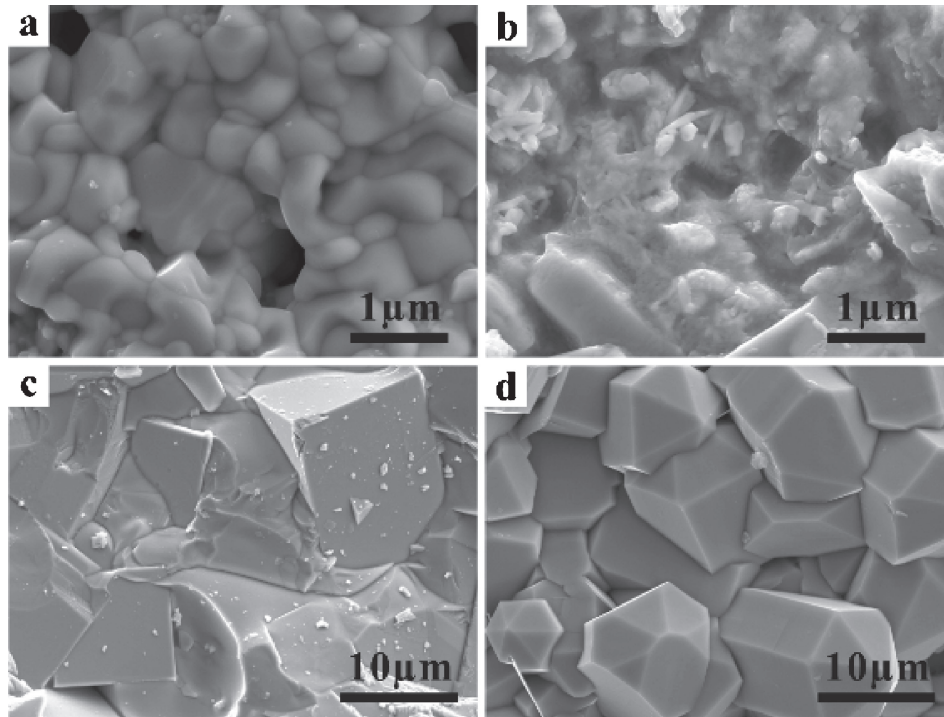
Fig. 3. Cross-sectional SEM pictures of pressureless sintered BZCY pellets before (a) and after (b) HPHS test, and high-pressure sintered BZCY pellets before (c) and after (d) HPHS test.
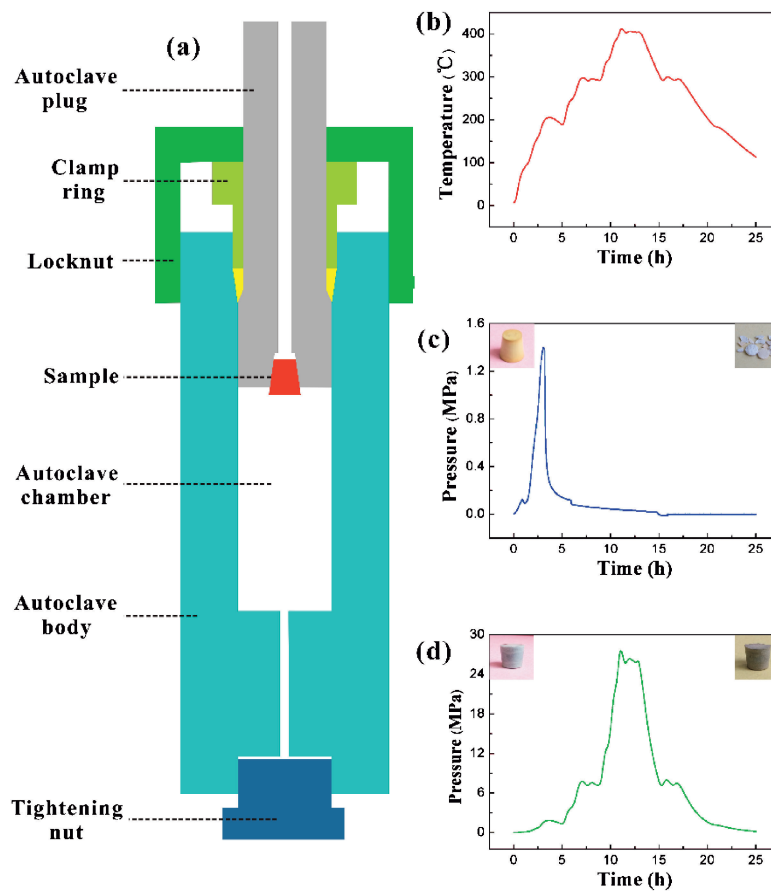

Fig. 4. (a) Schematic diagram of the experimental setup for HPHS test, (b) temperature in autoclave vs. recording time and pressure in autoclave vs. recording time when pressureless sintered BZCY sample (c) and high-pressure sintered BZCY sample (d) were used as sealing materials during HPHS test.

JCS-Japan

the sample, and then gradually expand to the interior with time until the sample breaks. Unlike pressureless sintered BZCY, there are hardly any obvious large pores in the high-pressure sintered BCZY sample, and only a few closed pores may exist. These small pores are not connected, so only part of pores on the surface may collapse under stress corrosion rather than the sample breaks. The results show that the pressureless sintered BZCY sample cannot be used in HPHS because it unable to withstand the impact of high-pressure hydrothermal fluid, while the high-pressure sintered BZCY sample appears not to be affected by high-pressure hydrothermal fluid, making it potentially suitable for use in HPHS.

$BaZr_{0.7}Ce_{0.2}Y_{0.1}O_{3-\delta}$ ceramic was successfully sintered via high-pressure sintering method at 1200°C/1 GPa. A comparative research of pressureless sintering and high-pressure sintering methods was carried out by using a series of tests and characterization techniques. High-pressure sintering accelerated the sintering densification resulting in compact and uniform microstructure with micron-sized grains and no porosity and crack, which guaranteed high performance of products. The HPHS test results show that high-pressure sintered BZCY sample appears not to be affected by high-pressure hydrothermal fluid, while pressureless sintered BZCY sample cannot be used in HPHS due to its poor resistance to pressure and corrosion. Based on the above-mentioned achievements in research, high-pressure sintering technique emerges as a promising method to prepare high performance BZCY ceramic and overcome the major obstacles related to practical applications in HPHS.

References

1) N. Kochetova, I. Animitsa, D. Medvedev, A. Demin and P. Tsiakaras, *RSC Adv.*, **6**, 73222–73268 (2016).
2) E. Fabbri, D. Pergolesi and E. Traversa, *Chem. Soc. Rev.*, **39**, 4355–4369 (2010).
3) T. Ishiyama, H. Kishimoto, K. Develos-Bagarinao, K. Yamaji, T. Yamaguchi and Y. Fujishiro, *J. Ceram. Soc. Jpn.*, **125**, 247–251 (2017).
4) J. Zamudio-Garcia, J. M. Porras-Vazquez, L. dos Santos-Gomez, E. R. Losilla and D. Marrero-Lopez, *Ceram. Int.*, **44**, 14113–14121 (2018).
5) Y. S. Du, J. F. Xia, H. Q. Nian, G. H. Zhou, D. Y. Jiang and Q. Li, *J. Ceram. Soc. Jpn.*, **125**, 520–523 (2017).
6) G. S. Reddy and R. Bauri, *J. Alloy. Compd.*, **688**, 1039–1046 (2016).
7) L. Bi, E. H. Da'as and S. P. Shafi, *Electrochem. Commun.*, **80**, 20–23 (2017).
8) N. Bausá, S. Escolástico and J. M. Serra, *J. CO₂ Util.*, **34**, 231–238 (2019).
9) G. Heras-Juaristi, D. Pérez-Coll and G. C. Mather, *J. Power Sources*, **364**, 52–60 (2017).
10) Á. Triviño-Peláez, D. Pérez-Coll and G. C. Mather, *Acta. Mater.*, **167**, 12–22 (2019).
11) K. Ding and W. E. Seyfried, *Chem. Rev.*, **107**, 601–622 (2007).
12) M. D. Goncalves, P. S. Maram, A. Navrotsky and R. Muccillo, *Ceram. Int.*, **42**, 13689–13696 (2016).